Food Chemistry 355 (2021) 129666

Contents lists available at ScienceDirect

Food Chemistry

journal homepage: www.elsevier.com/locate/foodchem

A novel aptasensing method for detecting bisphenol A using the catalytic effect of the Fe_3O_4/Au nanoparticles on the reduction reaction of the silver ions

Fatemeh Farahbakhsh [a], Esmaeil Heydari-Bafrooei [b,*], Mehdi Ahmadi [a], Seyedeh Hoda Hekmatara [a], Mohammad Sabet [b]

[a] Department of Physics, Vali-e-Asr University of Rafsanjan, 77188–97111, Iran
[b] Department of Chemistry, Vali-e-Asr University of Rafsanjan, 77188–97111, Iran

ARTICLE INFO

Keywords:
Bisphenol A
Aptamer
Magnetic nanoparticles
Biosensor
Stripping differential pulse voltammetry

ABSTRACT

The gold electrode was functionalized with anti-bisphenol A (BPA) aptamer and captured the BPA as analyte. By dropping the aptamer-modified magnetic Fe_3O_4/Au nanoparticles solution onto the electrode, a BPA molecule attaches to many aptamers that are in contact with a large number of Fe_3O_4/Au nanoparticles. The modified electrode were transferred to a solution containing Ag^+ ions. Fe_3O_4/Au nanoparticles reduce the Ag^+ ions to Ag^0. A potential scan was applied for the oxidation of the Ag^0-loaded magnetic nanoparticles to the AgCl. The magnitude of the stripping anodic signal of the Ag^0 was related to the concentration of the BPA. The assay shows a detection limit of 0.6 fmol L^{-1} and linear range of 1 fmol L^{-1}-150 pmol L^{-1} and. The applicability of the aptasensor is measured by its successful use in the sensing BPA in water, milk and juice samples and measuring BPA migration from different commercial plastic products.

1. Introduction

Bisphenol A (BPA) is an endocrine-disrupting chemical, which has severe health damage (Huang et al., 2020; Jiang et al., 2020). BPA is widely used in the manufacture of epoxy/polycarbonate resin products, which are considerably used in water bottles, baby bottles, plastic food containers and in the manufacture of compact discs and medical devices (Khanmohammadi et al., 2020). BPA can be released into surface water via wastewater of industries that manufactures plastic materials. Therefore, it is greatly needed to propose a selective analysis procedure for monitoring BPA in the different real samples. Various techniques have been proposed for the measurement of BPA, including colorimetry (Lee, Lee, Kim, & Lee, 2019), high-performance liquid chromatography (Zhao et al., 2019), LC-MS/MS (Dreolin, Aznar, Moret, & Nerin, 2019), field-effect transistor (Liu et al., 2018), electrochemiluminescence (Zhang et al., 2019), fluorescence (Yun, Wu, Chen, & Yang, 2018), GC–MS (Johnson, Burke, Harrison, & Burdette, 2012) and electroanalytical methods (Alam & Deen, 2020; Ekomo et al., 2018; Mahmoudi et al., 2019). In this regard, most researchers are focusing on the use of electrochemical biosensors for BPA detection (Qin et al., 2018; Ashraf et al., 2019; Baghayeri et al., 2018; Deiminiat et al., 2017; Yu et al., 2019; Beiranvand et al., 2017; Liu et al., 2016; Li et al., 2019; Ensafi et al., 2018; Zhang et al., 2021; Xu et al., 2020; nodehi et al., 2021; Messaoud et al., 2018). Biosensors work on the basis of an affinity reaction between a immobilized biomolecule and target molecule (BPA). As a result, a physical signal generates and the analyte concentration detects by evaluating of the signal. The physical signal in electrochemical biosensors is an electrochemical response.

Aptamers are single-stranded DNA and RNA or peptide molecules that are capable of specifically binding a target molecule. In recent years, aptamers have received a lot of attention because they not only have the benefits of antibodies, but also provide thermal stability, low cost, and a wide variety of applications. A range of analytical methods was linked to aptamer-based analysis including, fluorescence, quartz crystal microbalance, colorimetry, circular dichroism, optical transduction, surface plasmon resonance, atomic force microscopy and electrochemistry (Lee et al., 2017; Ren et al., 2019; Rajabnejad et al., 2020). If the aptamer is used as a bioreceptor in a sensor, it is called an aptasensor.

There are two detection platforms for aptasensors: single aptamer-

* Corresponding author.
E-mail address: e.heydari@vru.ac.ir (E. Heydari-Bafrooei).

https://doi.org/10.1016/j.foodchem.2021.129666
Received 20 June 2020; Received in revised form 13 March 2021; Accepted 17 March 2021
Available online 23 March 2021

based biosensors and sandwich-type aptamer-based biosensors 31. (Seo & Gu, 2017). In a single aptamer-based biosensor, the target molecule bind to the aptamer that is immobilized on the transducer and the detection was performed by monitoring a physical signal (Heydari-Bafrooei & Askari, 2017; Rostamabadi & Heydari-Bafrooei, 2019; Mohammadi et al., 2020). Single aptamer-based biosensors suffered from their low sensitivities, and making it approximately impossible to get these sensors into the practical and commercial stage. To overcome this drawback, as an alternative, sandwich-type aptasensors utilizing a couple of antibody complex and/or aptamer have been established. In a double-aptamer sandwich assay, two aptamers are employed, the first is the capture probe and the second is a reporter probe. The capture probe is immobilized on a suitable solid substrate such as electrodes and nanoparticles, thereby trapped the target molecule. Then the reporter probe, which is usually attached to a signaling molecule such as enzymes or nanoparticles, is bound to the target molecule. Simultaneous attachment of two aptamers in double-aptamer sandwich assays makes them as a very selective aptasensing method for direct analysis of complex samples, such as blood serum and environmental samples.

Herein, considering the advantages of the double-aptamer sandwich assay, we designed an electrochemical aptasensor for sensitive quantitative sensing of BPA. Magnetic gold nanoparticles (Fe_3O_4/Au nanoparticles) were synthesized to exploit as signal amplifiers. Each Fe_3O_4/Au nanoparticle was attached to a large number of the aptamer specific to BPA (Fe_3O_4/Au-aptamers nanoparticles). BPA was captured by the aptamer on a gold electrode, and then recognized by the Fe_3O_4/Au-aptamer complex. This procedure let numerous Fe_3O_4-Au nanoparticles to be immobilized on the surface of the electrode. The Fe_3O_4/Au nanoparticles were dissolved by HNO_3 and dispersed into the solution containing Ag^+ ions. The remaining hydroxylamine groups on the Fe_3O_4/Au nanoparticles can reduce the Ag^+ ions to Ag^0. Due to alkaline conditions, the Ag_2O was also produced in the medium. Anyway, Ag^+ and Ag_2O accumulated on the Fe_3O_4/Au nanoparticles surface. The magnetic nanoparticles were transported to the electrode surface and the deposited Ag_2O was electrochemically reduced to Ag^0. Finally, the Ag^0 was oxidized to AgCl by using stripping differential pulse voltammetry (SDPV). The BPA concentration was sensed based on the current signal of the stripping voltammogram of the oxidation of the Ag^0 to AgCl.

2. Materials and methods

2.1. Materials and apparatus

BPA, 6-mercapto-1-hexanol, Chloroauric acid ($HAuCl_4$, 99.9%) and $K_3[Fe(CN)_6]/K_4[Fe(CN)_6]$ were purchased from Sigma-Aldrich, St. Louis, MO. All other reagents were of analytical grade and obtained from Merck Chemicals KGaA, Darmstadt, Germany. Thiol-terminated 63-mer BPA aptamer (5′-SH-$(CH_2)_6$-CCG-GTG-GGT-GGT-CAG-GTG-GGA-TAG-GGT-TCC-GCG-TAT-GGC-CCA-GCG-CAT-CAC-GGG-TTC-GCA-CCA-3′) was acquired from Bioneer Corporation, Daejeon, Korea. The aptamer solution was prepared in Tris-HCl buffer and was kept in the freezer before use. The concentration and pH of the Tris-HCl buffer is 10 mmol L^{-1} and 7.4, respectively. The solutions of the Ag^+ ion were made from their nitrate salt. All samples were characterized by transmission electron microscopy (TEM, Tecnai G2 20ST), UV–Vis spectroscopy (Agilent Cary 60 UV–vis spectrophotometer), scanning electron microscopy (SEM, JEOLJSM-7600F), and vibrating sample magnetometry (VSM, Princeton MICROMAG 3900).

2.2. Synthesis of Fe_3O_4 nanoparticles

The synthesis of Fe_3O_4 nanoparticles is in accordance with the method previously described by our group (Farahbakhsh et al., 2019). $FeCl_2{\cdot}6H_2O$ and $FeCl_3{\cdot}6H_2O$ with 0.98:2.703 g ratios were dissolved in 100 mL deionized water at 80 °C temperature. The solution was stirred vigorously for 30 min until the salts are dissolved. Then, 25 mL ammonia solution of 28% w/v% was added dropwise. The black solution was stirred for 30 min under N_2 gas at 80 °C temperature. Consequently, the black precipitation was washed and dried in an oven for 8 h.

2.3. Synthesis of Fe_3O_4/Au nanoparticles

The synthesis of Fe_3O_4/Au nanoparticles is according to the literature procedure (Zhang et al., 2011; Dadmehr et al., 2014). A solution containing 3 mL hydroxylamine hydrochloride (0.2 mol L^{-1}) and 10 mL of 1 mg mL^{-1} as-prepared Fe_3O_4 nanoparticles was diluted with 50 mL 0.03 mol L^{-1} tetramethylammonium hydroxide and heated to 80 °C, then, followed by the addition of 25 mL of 50 mmol L^{-1} sodium citrate solution and stirred for 30 min. One hundred ml of 0.2 mg mL^{-1} $HAuCl_4$ solution was added dropwise while the solution is vigorously stirred under N_2 gas. The change in the color of the precipitate from black to reddish-brown indicates the successful synthesis of the Au nanoparticles. The Fe_3O_4/Au nanoparticles were separated using a permanent magnet.

2.4. Synthesis of aptamer-modified Fe_3O_4/Au nanoparticles

The procedure for attachment of thiol-terminated BPA aptamer to Fe_3O_4/Au nanoparticles is according to the literature procedure (Zhang et al., 2011). Ten mg of as-prepared Fe_3O_4/Au nanoparticles was dispersed in 1.0 mL of 10 mmol L^{-1} Tris–HCl buffer (pH = 7.4) and then 20 μL of 100 μM aptamer was added to the nanoparticles suspension, and the mixture was mildly stirred for 24 h. The unbound aptamers were removed by a magnet. The magnetically separated nanoparticles were washed with double distilled water and Tris–HCl buffer four times and lastly were re-dispersed in 5 mL of Tris–HCl solution.

2.5. Aptamer-BPA assay

To clean the gold electrode (2.0 mm diameter, Metrohm), the electrode was rinsed in piranha solution for 60 s to remove the organic impurities. Then, the electrode washed twice with ethanol and water mixture (1:1). Afterward, the electrode surface was polished with aluminum oxide powder (grain size 0.3 μm), then rinsed thoroughly with water and sonicated 2 min into an ethanol/water mixture in a volume ratio of 1:1. The cleaned gold electrode was then transferred to an electrochemical cell containing 0.5 mol L^{-1} H_2SO_4 and the potential cycled between −0.2 to 1.5 V until a stable cyclic voltammogram was obtained. Ten μL of 2 μmol L^{-1} thiol-terminated BPA aptamer was dropped cast on the cleaned surface of the electrode and maintained overnight at the 4 °C. The electrode was immersed twice in water to eliminate additional aptamer molecules. Finally, unbound sites and non-specific adsorptions were blocked by casting of 5 μL of 3.0 μmol L^{-1} 6-mercapto-1-hexanol solution on the modified electrode for 0.5 h. After preparing the aptamer-functionalized gold electrode, 5 μL of BPA solutions with different concentrations dropped on the modified electrode and incubated on the electrode for 2 h at room temperature. Then, 5 μL of the Fe_3O_4/Au-aptamer complex was dropped and incubated on the surface for 1 h. After the electrode washing with Tris-HCl buffer, the Fe_3O_4/Au nanoparticles remaining at the surface of the electrode were dissolved by the addition of 100 μL of 0.10 mol L^{-1} HNO_3 solution.

2.6. Electrochemical detection

The Fe_3O_4/Au nanoparticles released from the electrode surface were added into the solution containing 0.5 mmol L^{-1} Ag^+. The pH of the suspension was adjusted to 12.0 and the mixed solution was incubated for 180 s in ambient condition. The nanoparticles were separated from the medium by a magnet. Then, to remove the residual matrix, the Fe_3O_4/Au nanoparticles were washed with water four times. The Fe_3O_4/Au nanoparticles were captured on the gold electrode surface and then a

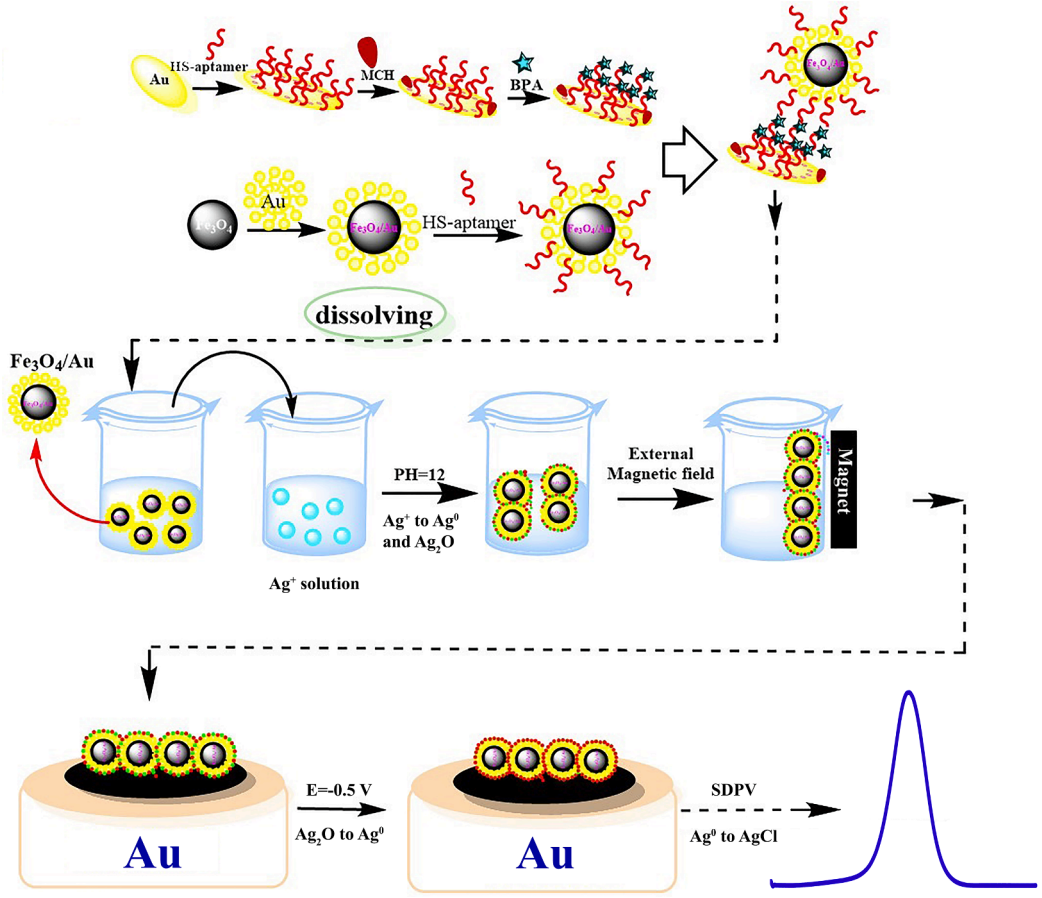

Fig. 1. Schematic illustration of the sensing mechanism of the aptasensor for the detection of BPA.

constant potential of −500 mV was applied to the electrode for 3 min in 0.1 mol L^{-1} KCl solution (pH = 7.0) to reduce the deposited Ag_2O on the Fe_3O_4/Au nanoparticles surface to Ag^0. Finally, the Ag^0 was oxidized to AgCl by using SDPV. the modified electrode was transferred to an electrochemical cell containing 0.1 mol L^{-1} KCl solution (pH = 7.0). The DPV was achieved with a potential scan from − 0.2 to 0.6 V in a pulse width of 50 ms and a pulse amplitude of 50 mV. The electrochemical analysis was performed by Autolab PGSTAT204 with NOVA 2.1 software. A three-electrode system containing a Pt wire, Ag|AgCl|3.0 M KCl and gold electrode as the auxiliary, reference and working electrode was used.

2.7. Real samples preparation

Tap and river waters were acquired from our laboratory in Rafsanjan (Iran) and Zayandehroud River in Isfahan (Iran), respectively. Different volumes of the standard solution of BPA were spiked to water samples and the recovery percentages were reported. A Whatman No. 45 filter paper was used to filtrate water samples. A 5-fold dilution factor was selected for the samples. Mineralized water, orange juice and milk sample acquired from a supermarket in Rafsanjan (Iran). These samples were also spiked with various volumes of BPA. To eliminate the upper suction fat, the milk sample was centrifuged at 6,000 × g for 20 min. The proteins were precipitated by mixing up the equivolume of the milk sample and ethanol and centrifugation at 6,000 × g for 10 min. The supernatant was filtrated and diluted 5-fold with water. For the orange juice, after ultrafiltration with a 0.22-μm membrane, the solution was diluted 10-fold with water.

2.8. Bottle samples pretreatment for migration tests

In October 2020, several plastic bottles and food containers that may contain BPA, including baby feeding bottles, plastic flasks and plastic jars were collected from local stores in Iran. The total volume of the bottles was filled with acetonitrile or with food simulants (distilled water; ethanol, 50% v/v; acetic acid, 3% w/v). 3% of acetic acid in water is the simulant for acidic foods (e.g., fruit juice) and 50% ethanol in water is the food simulant for milk products (e.g., infant formula) (EEC, 1985). A water bath was prepared at a temperature of 60 °C and the bottles filled with acetonitrile were placed in it for 24 h and then allowed to cool at room temperature. The bottles full of food simulants were also placed in the bath at 40 °C for 10 days. For all these conditions, the samples were wrapped in aluminum foil to avoid photolysis due to exposure to light. The extract was then evaporated to dryness under reduced pressure in a rotary evaporator with nitrogen steam at 40 °C. Reconstitution of the dried extract was performed by 20 mL acetonitrile (three times) and after mixing, the total extract kept at refrigerator temperature (2–4 °C) before assay. A standard addition approach was used for the determination of the BPA after dilution of a certain amount of the samples with Tris–HCl buffer (10 mmol L^{-1}, pH 7.4).

3. Results and discussion

Magnetic gold nanoparticles (Fe_3O_4/Au nanoparticles) herein were used for two purposes; first, to amplify the signal, and second to catalyze the reduction of Ag^+. Due to the nanosize structure of Fe_3O_4/Au, a large amount of the BPA-specific aptamers on the surface of the electrode were attached to each Fe_3O_4/Au nanoparticle and led to the immobilization of numerous Fe_3O_4-Au nanoparticles. The Fe_3O_4/Au

nanoparticles can cause catalysis reduction of Ag^+ ions to Ag^0. Therefore, by dissolving the immobilized nanoparticles and putting them in contact with Ag^+ ions and monitoring the progress of the reduction reaction of Ag^+ by using SDPV, the concentration of BPA was determined. Furthermore, the presence of gold nanoparticles on the Fe_3O_4 particles is necessary for immobilization of thiol-terminated BPA aptamer by covalent bonds Au-S.

3.1. Schematic illustration

Fig. 1 illustrates the preparation and the sensing mechanism of the electrochemical aptasensor for the detection of BPA. The procedure is based on the use of magnetic nanoparticles for signal amplification and catalytic effect on the reduction of Ag^+. Thiol-terminated BPA aptamer was immobilized on the gold electrode by covalent bonds Au-S. 6-mercapto-1-hexanol was applied to block unbound sites and non-specific adsorptions. The aptamer-modified electrode selectively recognizes the BPA molecule. In another experiment, thiol-terminated BPA aptamers were attached to many Fe_3O_4/Au nanoparticles by covalent bonds Au-S. By dropping aptamer-loaded Fe_3O_4/Au nanoparticles on the aptamer-modified electrode (after interaction with BPA), a molecule of BPA can attach to many Fe_3O_4/Au nanoparticles. This step leads to thousands of times amplification of the signal and the ultra-trace determination of BPA. The Fe_3O_4/Au nanoparticles on the surface of the electrode were dissolved by HNO_3 and were added into the solution containing Ag^+. The remaining hydroxylamine groups on the Fe_3O_4/Au nanoparticles surface can reduce the Ag^+ ions to Ag^0. On the other hand, in this experiment, the Fe_3O_4/Au nanoparticles is a catalyst for the reduction of Ag^+. Typically, during this process, due to the alkaline condition, the Ag_2O was also produced in the medium. Anyway, Ag^0 and Ag_2O accumulated on the Fe_3O_4/Au nanoparticles surface. The magnetic nanoparticles were transported to the surface of the gold electrode and then by applying a constant potential of −500 mV for 180 s, the deposited Ag_2O on the Fe_3O_4/Au nanoparticles surface reduce to Ag^0. Lastly, a positive-going differential pulse potential scan was applied to oxidate the Ag^0 to the AgCl. The magnitude of the stripping anodic signal of the Ag^0 was related to the concentration of the BPA. By an increase in the concentration of BPA in the solution, the amount of the BPA on the surface of the aptamer-modified electrode increases, and consequently, the amount of the aptamer-modified Fe_3O_4/Au nanoparticles that were attached to the BPA increases and finally, the quantity of the available Fe_3O_4/Au nanoparticles for the reduction of the Ag^+ ions to Ag^0 increases. Therefore, by the increase in the number of Fe_3O_4/Au nanoparticles, the amount of the preconcentrated Ag^0 on the Fe_3O_4/Au nanoparticles surface increases and consequently, the current of the stripping voltammogram of the oxidation of the Ag^0 to AgCl increases.

3.2. Surface characterization

Figure S4 displays the Nyquist plots of the electrode for the characterization of the interfacial changes in the stepwise assembly process of the aptasensor. The equivalent circuit was shown in Figure S5. When the gold electrode was modified with the aptamer (curve b) and the BPA (curve c), the charge transfer resistance (R_{ct}) increased compared to the bare electrode (curve a), due to hindering effect of the aptamer and BPA molecules. After binding of the Fe_3O_4/Au-aptamer to the BPA, the R_{ct} was also increased (curve d) due to the more blocking and insulation effect, which initiates from hampered mass transport and electron transfer.

3.3. Electrochemical investigation of the deposition of silver on the surface of Fe_3O_4/Au nanoparticles

To assess the ability of the dissolved Fe_3O_4/Au nanoparticles from the surface of the electrode to capture the Ag^+, CV and DPV of the gold electrode was investigated. For this purpose, two experiments was performed according to the procedure presented in sections 2–5 and 2–6. In experiment 1, the released Fe_3O_4/Au nanoparticles from the surface of the electrode were not treated with Ag^+ solution and directly transferred on the surface of the gold electrode. But, in the experiment of 2, Fe_3O_4/Au nanoparticles after dissolving were added in a solution with a pH value of 12 containing 1 mmol L^{-1} Ag^+ and the mixture was incubated for 180 s at room temperature. Then the magnetic nanoparticles are

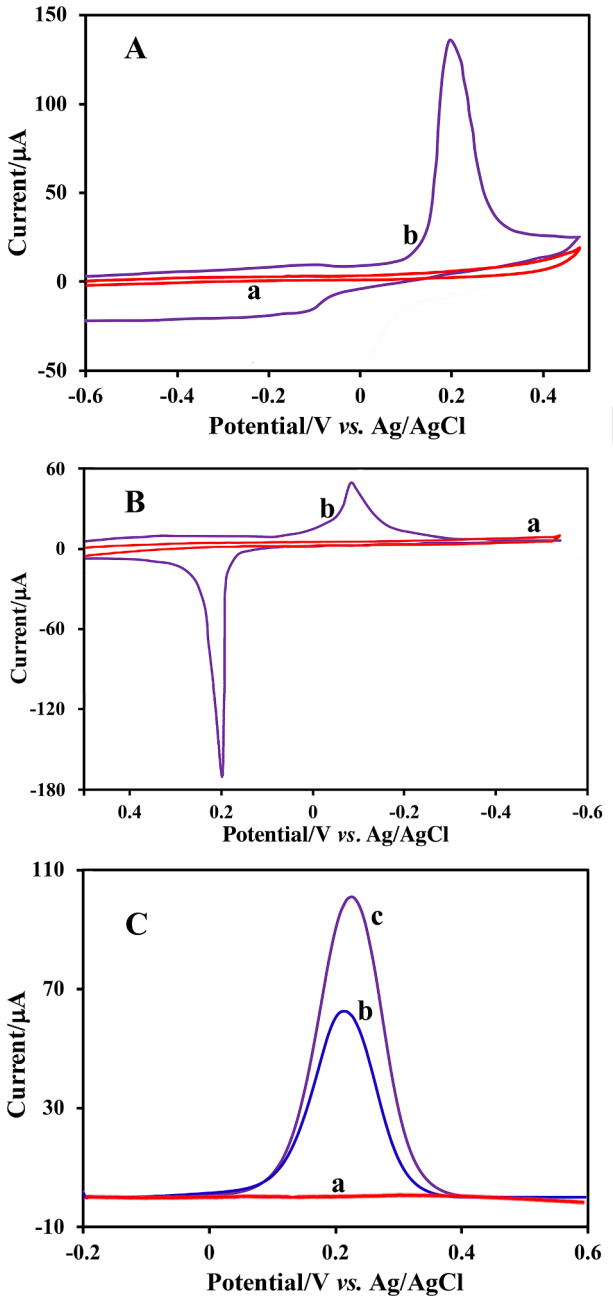

Fig. 2. (A) and (B) cyclic voltammetric curves of Fe_3O_4/Au nanoparticles-modified gold electrodes. The Fe_3O_4/Au nanoparticles were not incubated (a) and incubated (b) in the Ag^+ solution. (C) DPV of the Fe_3O_4/Au nanoparticles-modified gold electrodes. The Fe_3O_4/Au nanoparticles were not incubated (a) and incubated (b & c) in the Ag^+ solution. After incubating the Fe_3O_4/Au nanoparticles in Ag^+ solution, the Fe_3O_4/Au nanoparticles-modified gold electrode was treated with (b)/without (c) electrochemical reduction. Detection solutions were 0.1 mol L^{-1} KCl (pH = 7.0). reduction voltage, −500 mV; reduction time, 180 s; concentration of $AgNO_3$, 1000 μmol/L; incubation time, 180 s; scan rate, 50 mV/s; concentration of BPA, 30 pmol L^{-1}.

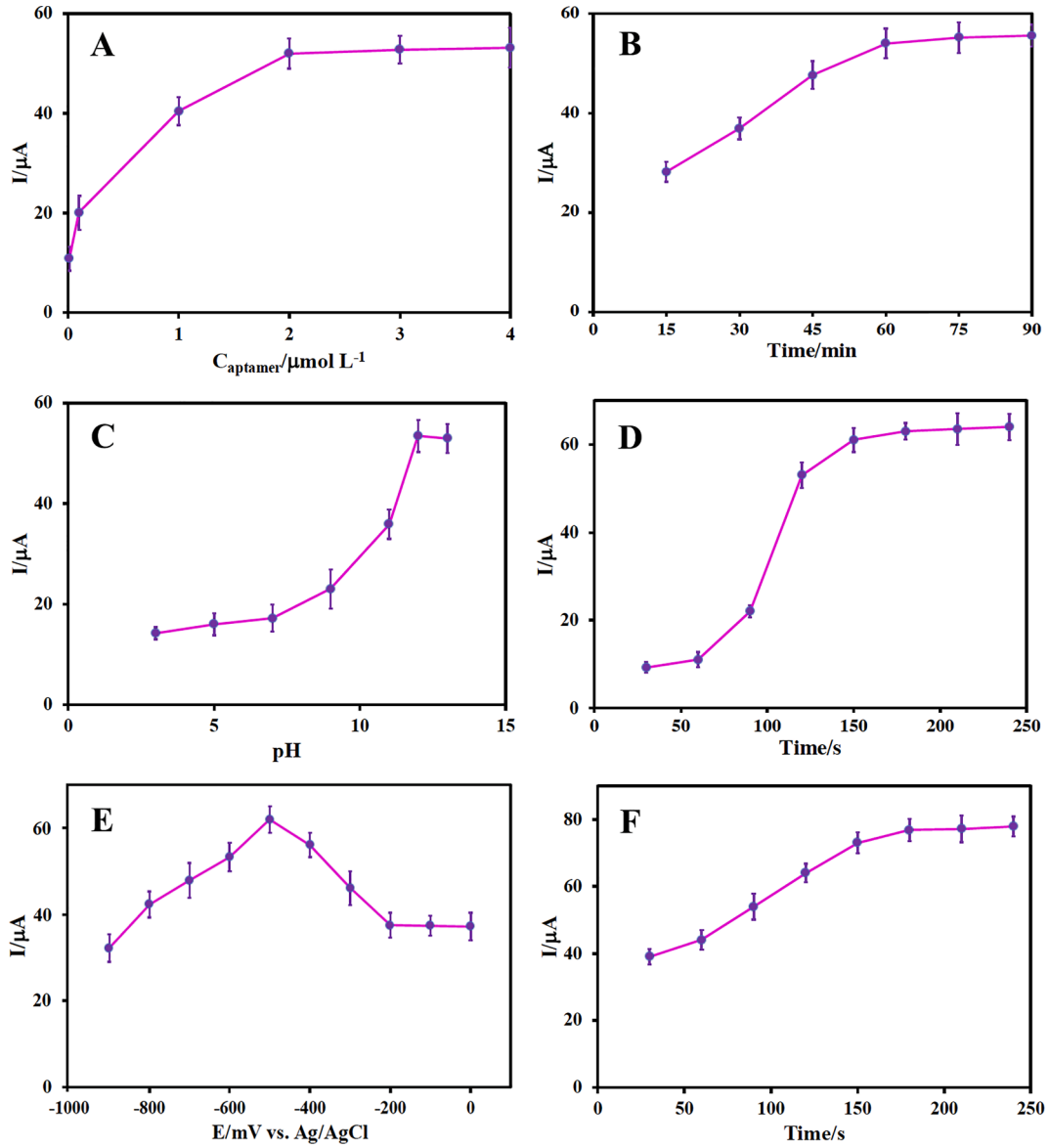

Fig. 3. Effects of the aptamer concentration (A), incubation time of the Fe_3O_4/Au-aptamer on the surface of the electrode (B), pH of the Ag^+ solution (C), incubation time of the Fe_3O_4/Au nanoparticles in Ag^+ solution (D), time (E) and potential (F) of the reduction of the Ag_2O to Ag^0 on the stripping current of Ag^0 in 0.1 mol L^{-1} KCl.

transported to the gold surface of the electrode. Fig. 2A displays CV of the electrode without (a) and with (b) interaction of released Fe_3O_4/Au nanoparticles with Ag^+ in 0.1 mol L^{-1} KCl solution (pH = 7.0). The CV of the electrode covered with untreated Fe_3O_4/Au nanoparticles shows no oxidation and/or reduction signals. A clear oxidation peak was seen in the case of the electrode covered with interacted Fe_3O_4/Au nanoparticles with Ag^+, which is attributed to oxidation of Ag^0 to AgCl in 0.1 mol L^{-1} KCl (Singh et al., 2012). As a result, Fe_3O_4/Au nanoparticles can capture the Ag^+ as Ag^0. The reduction of Ag^+ to Ag^0 is because of the presence of the remaining hydroxylamine groups on the surface of Fe_3O_4/Au nanoparticles as the reducing agent, which is used in the synthesis of the Fe_3O_4/Au nanoparticles (Lai et al., 2011; Yang et al., 2013). Furthermore, the Fe_3O_4/Au nanoparticles also catalysis the process of adsorption/deposition of Ag^+ (Yang et al., 2013). The CV result shows that by combining of Ag^+ and Fe_3O_4/Au nanoparticles, the Ag^+ ion reduces to Ag and by the transportation of the silver-deposited Fe_3O_4/Au nanoparticles to the electrode surface, the stripping oxidation peak current of silver was observed.

In the negative scan direction, as shown in Figure 2B, a reduction peak was also observed at −0.085 V, which can be ascribed to the electroreduction of Ag_2O to Ag^0, as has been described in the literature (Singh et al., 2012). From this observation, it can be deduced that during the reduction of Ag^+ to Ag^0, due to the alkaline condition, the Ag_2O are also formed and deposited on the Fe_3O_4/Au nanoparticles surface. Therefore, before the stripping differential pulse voltammetry, the deposited Ag_2O reduces to Ag^0 by applying a constant potential of −500 mV for 3 min. By doing this, the quantity of Ag^0 increases and consequently, the oxidation signal of Ag^0 to AgCl improves, as shown in Fig. 2C.

3.4. Optimization of the experimental parameters

The effect of different parameters on the sensitivity of the sensor was divided to seven sections, including the optimization of the concentration of the aptamer, the incubation time of the Fe_3O_4/Au-aptamer on the surface of the electrode, the effect of the pH on the reduction of Ag^+ to Ag^0, the incubation time of the magnetic nanoparticles in Ag^+ solution, the time and the potential of the reduction of the Ag_2O to Ag^0 and the

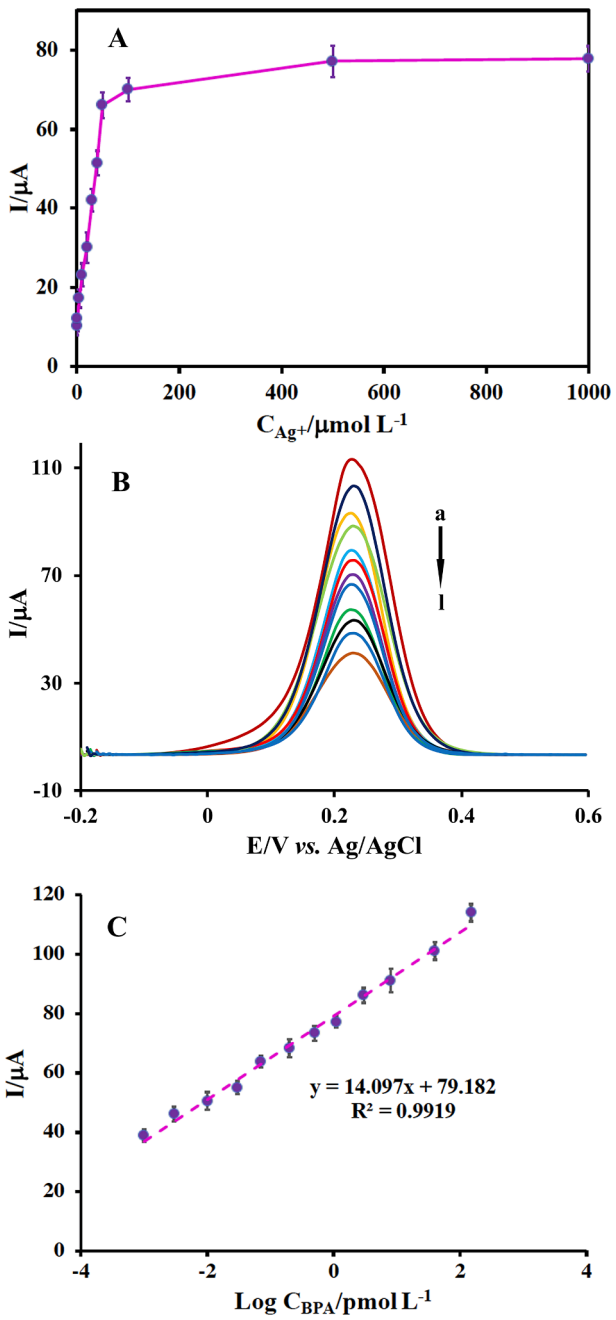

Fig. 4. (A) Effect of $AgNO_3$ concentration on the stripping current of Ag^0 in 0.1 mol L^{-1} KCl. (B) Stripping differential pulse voltammetric curves of Ag^0 immobilized at the Fe_3O_4/Au modified gold electrode and (C) the linear calibration plot for determination of BPA. The concentrations of BPA varied as (a) 0.001, (b) 0.003, (c) 0.01, (d) 0.03, (e) 0.07, (f) 0.2, (g) 0.5, (h) 1.1, (i) 3, (j) 8, (k) 40 and (l) 150 pmol L^{-1}.

concentration of Ag^+. For this purpose, the stripping anodic current of Ag^0 to AgCl is checked as a function of the experimental parameters.

For finding the optimum concentration of the anti-BPA aptamer, the concentration was changed in the range from 0.01 to 4 µmol L^{-1}. As shown in Fig. 3A, the stripping anodic current of Ag^0 increased till 2 µmol L^{-1} and then leveled off. The incubation time of the Fe_3O_4/Au-aptamer on the electrode surface was also explored. It can be seen in Fig. 3B, the maximum stripping anodic current of Ag^0 was achieved when the incubation time is 60 min.

To assess the effect of the pH on the reduction of Ag^+ to Ag^0, the pH of the solution in the range of 4.0 to 14.0 was investigated. As shown in Fig. 3C, during the increasing of the pH, the current for stripping oxidation of Ag^0 to AgCl was enhanced till pH = 12 and then it was approximately leveled off in longer pHs. Therefore, it can be concluded that at pH above 12, the Ag^+ ions almost entirely deposit on the Fe_3O_4/Au nanoparticles surface as Ag^0. Accordingly, pH 12.0 was chosen for all subsequent trials.

The efficiency of the reduction of Ag^+ to Ag^0 depends on the incubation time of the Fe_3O_4/Au nanoparticles in the Ag^+ solution. For this purpose, the stripping oxidation current of Ag^0 to AgCl was evaluated and attained in the range of 30–240 s as the incubation time. As shown in Fig. 3D, the signal reaches a constant value after about 180 s incubation. It found that the optimum time for the total reduction of Ag^+ ions and deposition of Ag^0 on the Fe_3O_4/Au nanoparticles surface is 180 s. The Ag_2O that co-deposited with Ag^0 on the surfaces of the magnetic nanoparticles must be reduced to Ag^0 by applying an appropriate potential before stripping differential pulse oxidation of Ag^0 to AgCl. The experimental conditions, including the potential and the time of Ag_2O reduction, were optimized. The reduction potential and time were changed from 0 mV to −900 mV and 30–240 s, respectively. As shown in Fig. 3E & F, the maximum stripping signal obtained at − 500 mV and 180 s, which were selected for succeeding assays.

To investigate the effect of the concentration of Ag^+, eleven solution containing different concentrations of Ag^+ (with a pH value of 12) in the range of 0.1 to 1000 µmol L^{-1} was selected and the whole procedure steps were performed on each of these solutions separately and finally, the stripping oxidation current of Ag^0 to AgCl was evaluated. As shown in Fig. 4A, by the increase in the Ag^+ concentration to 1000 µmol L^{-1}, the intensity of the oxidation peak current of Ag^0 was increased. According to the results, the Ag^+ concentration was determined 500 µmol L^{-1} for assay of all solutions.

3.5. Characterization of the aptasensor

As explained above, it was proved that the complex of Fe_3O_4/Au nanoparticles attaches fine on the electrode. So, Fe_3O_4/Au nanoparticles can be dissolved with HNO_3, and used as a reductant to reduce Ag^+ to Ag^0. The formed Ag^0 were electrochemically oxidized to AgCl and stripped from the surface of the Fe_3O_4/Au nanoparticles. The stripping oxidation current of the Ag^0 can be used to indicate the level of BPA indirectly. As presented in Figure 4B, a clear stripping voltammetric peak can be seen at about 0.21 V for the oxidation of Ag^0. As shown in Fig. 4B and Figure S6, by an increase in the concentration of BPA, the intensity of the peak current increases. The dependence of the stripping current of the oxidation of Ag^0 to AgCl with the log of BPA concentration was displayed in Fig. 4C, which yields a linear plot. The calibration curve is linear in the range of 1 fmol L^{-1} to 150 pmol L^{-1}. The limits of detection of the assay was calculated to be 0.6 fmol L^{-1} at a signal-to-noise of 3. Table S1 compares the LOD and linearity of the method with the before published electrochemical aptamer-based methods for the determination of BPA. As shown in Table S1, the sensitivity of the method is comparable with others. Our research established a different approach for aptasensing of BPA, which applied magnetics nanoparticles and stripping voltammetric analysis for signal enhancement.

To investigate the selectivity of the sensor, the signal of the BPA aptasensor was measured by adding other molecules that may be present together with the analyte in real samples to the test solution. It was found that the presence of 100-fold of 2,6 dichlorophenol, p-benzoquinone, 4-nitrophenol, hydroquinone, indophenol, 4 aminothiophenol and p-nitrophenol and 50-fold of tetrabromobisphenol A has no meaningful effect on the BPA analysis. The results display an acceptable selectivity for ultra-trace determination of BPA.

The reproducibility of the sensor is an critical factor in the applicability of the sensor in real sample analysis. Therefore, the assay for the determination of 1 pmol L^{-1} of BPA was performed eight times. The relative standard deviation of 5.5% indicates good reproducibility of the method in measuring BPA.

Table 1
Recovery of BPA in spiked samples (n = 5).

Samples	Spiked (pmol L^{-1})	Proposed method			LC-MS-MS			F[b]	t[c]
		Found (pmol L^{-1})	Recovery% ± RSD[a]%	Bias %	Found (pmol L^{-1})	Recovery% ± RSD%	Bias %		
Tap water	0	ND[d]	–	–	ND	–	–		
	0.050	0.0476	95.2 ± 6.1	−4.8	0.0512	102.4 ± 4.9	2.4	1.339	2.098
	0.50	0.542	108.4 ± 4.7	8.4	0.547	109.4 ± 4.8	9.4	1.062	0.306
Zayandehrood River water	0	ND	–	–	ND	–	–		
	0.050	0.0530	106.0 ± 5.1	6.0	0.0526	105.2 ± 5.5	5.2	1.056	0.226
	0.50	0.473	94.6 ± 5.9	−5.4	0.470	94.0 ± 5.4	−6.0	1.209	0.167
Mineralized water	0	ND	–	–	ND	–	–		
	0.050	0.0518	103.6 ± 4.9	3.6	0.0491	98.2 ± 3.9	−1.8	1.757	1.899
	0.50	0.490	98.0 ± 6.4	−2.0	0.520	104.0 ± 4.7	6.0	1.646	1.688
Milk	0	ND	–	–	ND	–	–		
	0.050	0.0488	96.0 ± 4.9	−4.0	0.0512	102.4 ± 5.1	2.4	1.232	1.581
	0.50	0.519	103.8 ± 5.6	3.8	0.489	97.8 ± 5.0	−2.2	1.239	1.766
Orange juice	0	ND	–	–	ND	–	–		
	0.050	0.0532	106.4 ± 6.0	6.4	0.0527	105.4 ± 6.1	5.1	1.014	0.247
	0.50	0.527	105.4 ± 4.7	5.1	0.541	108.2 ± 5.5	8.2	1.193	0.854

Table 2
Migration of BPA from the plastic jar, plastic flask and baby bottle to 1 L acetonitrile (24 h @ 60 °C), distilled water (10 days @ 40 °C), 50% ethanol (10 days @ 40 °C) and 3% acetic acid (10 days @ 40 °C) as aqueous food simulant.

Sample	Migration solution	Proposed method		LC-MS-MS		F[b]	t[c]
		µg BPA	RSD[a] (%)	µg BPA	RSD (%)		
Plastic jar	Acetonitrile	7.911	4.7	8.343	3.9	1.306	1.237
	Distilled water	2.731	5.1	2.540	4.2	1.754	1.541
	50% ethanol	4.111	4.9	4.412	3.3	1.914	1.714
	3% acetic acid	3.323	5.5	3.519	4.7	1.221	1.126
Plastic flask	Acetonitrile	5.721	5.1	5.412	5.5	1.042	1.049
	Distilled water	1.102	6.2	1.018	3.1	3.953	1.722
	50% ethanol	3.612	4.3	4.065	5.1	1.783	2.476
	3% acetic acid	1.880	3.7	2.009	4.2	1.470	1.670
Baby bottle	Acetonitrile	1.119	6.2	0.986	5.9	1.422	2.080
	Distilled water	ND[d]	–	ND	–		
	50% ethanol	0.823	6.0	0.742	6.2	1.152	1.699
	3% acetic acid	ND	–	ND	–		

Aptasensor is an analytical tool and the storage stability of the devices are used for analytical purposes is very important, which should be clarified. Therefore, we tested the stability of the assay by comparing the signal obtained from the sensor that has been kept for 30 days at the refrigerator temperature with the newly prepared sensor. The results showed that the sensor can retain 95% of its first-day signal for 1 pmol L^{-1} BPA solution. The stability test shows that the sensor has acceptable stability.

The applicability of an analytical device is measured by its successful use in the determination of the analyte in real samples. Therefore, we studied the recovery of the spiked BPA in milk, fruit juice, tap, river and mineralized water samples. The results of the analysis have been presented in Table 1 and compared with those obtained using LC-MS-MS. There is no significant difference between the recoveries, relative standard deviation (RSD) and bias% obtained by the two methods. Variances of the two methods were compared with the F-test and considered no significantly different when $P > 0.05$. Statistical significance of differences in means was also tested by Student's *t*-test and conclude that there is no difference in means at the 95% confidence level.

The proposed method was applied to measure BPA migration from three commercial plastic products (plastic jar, plastic flask and baby bottle), and the results are described in Table 2. The results displayed that BPA was released from the plastic products to acetonitrile at 60 °C for 24 h and to distilled water, 50% ethanol and 3% acetic acid at 40 °C for 10 days. Migration solution affected the migration of BPA from bottles. The highest migration of BPA was found in acetonitrile. No significant BPA was found released from the baby bottles to distilled water and 3% acetic acid. The results of the analysis have been compared with those obtained using LC-MS-MS. The results of the two methods are in good agreement with each other and confirm the effectiveness of the assay for the analysis of real samples towards detection of BPA.

4. Conclusions

By considering the advantages of the double-aptamer sandwich assay and based on the catalytic effect of the Fe_3O_4-Au nanoparticles on the reduction reaction of Ag^+, a novel method utilizing magnetic nanoparticles for the aptasensing of BPA has been established. Simultaneous attachment of two aptamers to analyte in double-aptamer sandwich assays makes them as a very selective aptasensing method for analysis of complex samples. Although there are several published aptasensing methods for the analysis of different analytes by double-aptamer sandwich assay, here, in addition to the specific reaction of the analyte with aptamer, which is present in all aptasensors, we have used the catalytic properties of Fe_3O_4-Au nanoparticles for silver ion reduction reaction to increasing the sensitivity of the method. As can be seen in Table S1, this extra work significantly improves the LOD and linear dynamic range of the aptasensing methods. Comparison of the developed method with LC-MS-MS as a standard method for analysis of BPA in real samples showed that there is no significant difference in accuracy and precision between the two methods. However, this method has a large number of steps, representing the major limitation of the procedure. Nevertheless, although this extra work has increased the detection steps, it has dramatically enhanced the figures of merit for aptasensing detection of analytes. Therefore, the procedure can be suggested as a new method for electrochemical aptasensing assays of different molecules.

CRediT authorship contribution statement

Fatemeh Farahbakhsh: Methodology, Investigation, Formal analysis, Writing - original draft, Visualization, Software. **Esmaeil Heydari-Bafrooei:** Conceptualization, Validation, Resources, Writing - original draft. **Mehdi Ahmadi:** Supervision, Data curation, Funding acquisition. **Seyedeh Hoda Hekmatara:** Supervision, Data curation. **Mohammad Sabet:** Supervision, Data curation.

Declaration of Competing Interest

The authors declare that they have no known competing financial interests or personal relationships that could have appeared to influence the work reported in this paper.

Appendix A. Supplementary data

Supplementary data to this article can be found online at https://doi.org/10.1016/j.foodchem.2021.129666.

References

Alam, A. U., & Deen, M. J. (2020). Bisphenol A electrochemical sensor using graphene oxide and β-cyclodextrin-functionalized multi-walled carbon nanotubes. *Analytical Chemistry, 92*(7), 5532–5539. https://doi.org/10.1021/acs.analchem.0c0040210.1021/acs.analchem.0c00402.s001.

Ashraf, G., Asif, M., Aziz, A., Wang, Z., Qiu, X., Huang, Q., … Liu, H. (2019). Nanocomposites consisting of copper and copper oxide incorporated into MoS4 nanostructures for sensitive voltammetric determination of bisphenol A. *Microchimica Acta, 186*(6). https://doi.org/10.1007/s00604-019-3406-9.

Baghayeri, M., Ansari, R., Nodehi, M., Razavipanah, I., & Veisi, H. (2018). Voltammetric aptasensor for bisphenol A based on the use of a MWCNT/Fe3O4@gold nanocomposite. *Microchimica Acta, 185*, 320. https://doi.org/10.1007/s00604-018-2838-y.

Beiranvand, Z. S., Abbasi, A. R., Dehdashtian, S., Karimi, Z., & Azadbakht, A. (2017). Aptamer-based electrochemical biosensor by using Au-Pt nanoparticles, carbon nanotubes and acriflavine platform. *Analytical Biochemistry, 518*, 35–45. https://doi.org/10.1016/j.ab.2016.10.001.

Dadmehr, M., Hosseini, M., Hosseinkhani, S., Ganjali, M. R., Khoobi, M., Behzadi, H., … Sheikhnejad, R. (2014). DNA methylation detection by a novel fluorimetric nanobiosensor for early cancer diagnosis. *Biosensors and Bioelectronics, 60*, 35–44. https://doi.org/10.1016/j.bios.2014.03.033.

Deiminiat, B., Rounaghi, G. H., Arbab-Zavar, M. H., & Razavipanah, I. (2017). A novel electrochemical aptasensor based on f-MWCNTs/AuNPs nanocomposite for label-free detection of bisphenol A. *Sensors and Actuators B, 242*, 158–166. https://doi.org/10.1016/j.snb.2016.11.041.

Dreolin, N., Aznar, M., Moret, S., & Nerin, C. (2019). Development and validation of a LC–MS/MS method for the analysis of bisphenol a in polyethylene terephthalate. *Food Chemistry, 274*, 246–253. https://doi.org/10.1016/j.foodchem.2018.08.109.

EEC. (1985). Council directive of 19 December 1985 laying down the list of simulants to be used for testing migration of constituents of plastic materials and articles intended to come into contact with foodstuffs (85/572/EEC). *Official Journal of the European Communities, L372*, 14–21.

Ekomo, V. M., Branger, C., Bikanga, R., Florea, A.-M., Istamboulie, G., Calas-Blanchard, C., … Brisset, H. (2018). Detection of Bisphenol A in aqueous medium by screen printed carbon electrodes incorporating electrochemical molecularly imprinted polymers. *Biosensors and Bioelectronics, 112*, 156–161. https://doi.org/10.1016/j.bios.2018.04.022.

Ensafi, A. A., Amini, M., & Rezaei, B. (2018). Molecularly imprinted electrochemical aptasensor for the attomolar detection of bisphenol A. *Microchimica Acta, 185*, 265. https://doi.org/10.1007/s00604-018-2810-x.

Farahbakhsh, F., Ahmadi, M., Hekmatara, S. H., Sabet, M., & Heydari-Bafrooei, E. (2019). Improvement of photocatalyst properties of magnetic NPs by new anionic surfactant. *Materials Chemistry and Physics, 224*, 279–285. https://doi.org/10.1016/j.matchemphys.2018.11.074.

Heydari-Bafrooei, E., & Askari, S. (2017). Ultrasensitive aptasensing of lysozyme by exploiting the synergistic effect of gold nanoparticle-modified reduced graphene oxide and MWCNTs in a chitosan matrix. *Microchimica Acta, 184*(9), 3405–3413. https://doi.org/10.1007/s00604-017-2356-3.

Huang, M., Liu, S., Fu, L.i., Jiang, X., & Yang, M. (2020). Bisphenol A and its analogues bisphenol S, bisphenol F and bisphenol AF induce oxidative stress and biomacromolecular damage in human granulosa KGN cells. *Chemosphere, 253*, 126707. https://doi.org/10.1016/j.chemosphere.2020.126707.

Jiang, Y., Li, J., Xu, S., Zhou, Y., Zhao, H., Li, Y., … Xia, W. (2020). Prenatal exposure to bisphenol A and its alternatives and child neurodevelopment at 2 years. *Journal of Hazardous Materials, 388*, 121774. https://doi.org/10.1016/j.jhazmat.2019.121774.

Johnson, B. O., Burke, F. M., Harrison, R., & Burdette, S. (2012). Quantitative analysis of bisphenol a leached from household plastics by solid–phase microextraction and gas chromatography–mass spectrometry (SPME–GC–MS). *Journal of Chemical Education, 89*(12), 1555–1560. https://doi.org/10.1021/ed2003884.

Khanmohammadi, A., Jalili Ghazizadeh, A., Hashemi, P., Afkhami, A., Arduini, F., & Bagheri, H. (2020). An overview to electrochemical biosensors and sensors for the detection of environmental contaminants. *Journal of the Iranian Chemical Society, 17*(10), 2429–2447. https://doi.org/10.1007/s13738-020-01940-z.

Lai, G., Yan, F., Wu, J., Leng, C., & Ju, H. (2011). Ultrasensitive multiplexed immunoassay with electrochemical stripping analysis of silver nanoparticles catalytically deposited by gold nanoparticles and enzymatic reaction. *Analytical Chemistry, 83*(7), 2726–2732. https://doi.org/10.1021/ac103283p.

Lee, E.-H., Lee, S. K., Kim, M. J., & Lee, S.-W. (2019). Simple and rapid detection of bisphenol A using a gold nanoparticle-based colorimetric aptasensor. *Food Chemistry, 287*, 205–213. https://doi.org/10.1016/j.foodchem.2019.02.079.

Lee, E.-H., Lim, H. J., Lee, S.-D., & Son, A. (2017). Highly sensitive detection of bisphenol A by nanoaptamer assay with truncated aptamer. *ACS Applied Materials and Interfaces, 9*(17), 14889–14898. https://doi.org/10.1021/acsami.7b0237710.1021/acsami.7b02377.s001.

Li, H., Ding, S., Wang, W., Lv, Q., Wang, Z., Bai, H., & Zhang, Q. (2019). Voltammetric aptasensor for bisphenol A based on double signal amplification via gold-coated multiwalled carbon nanotubes and an ssDNA–dye complex. *Microchimica Acta, 186*, 860. https://doi.org/10.1007/s00604-019-4006-4.

Liu, S., Fu, Y., Xiong, C., Liu, Z., Zheng, L., & Yan, F. (2018). Detection of bisphenol A using dna-functionalized graphene field effect transistors integrated in microfluidic systems. *ACS Appl. Mater. Interfaces, 10*(28), 23522–23528. https://doi.org/10.1021/acsami.8b0426010.1021/acsami.8b04260.s001.

Liu, Y., Liu, Y., & Liu, B. (2016). A dual-signaling strategy for ultrasensitive detection of bisphenol A by aptamer-based electrochemical biosensor. *Journal of Electroanalytical Chemistry, 781*, 265–271. https://doi.org/10.1016/j.jelechem.2016.06.048.

Mahmoudi, E., Hajian, A., Rezaei, M., Afkhami, A., Amine, A., & Bagheri, H. (2019). A novel platform based on graphene nanoribbons/protein capped Au-Cu bimetallic nanoclusters: Application to the sensitive electrochemical determination of bisphenol A. *Microchemical Journal, 145*, 242–251. https://doi.org/10.1016/j.microc.2018.10.044.

Messaoud, N. B., Ait Lahcen, A., Dridi, C., & Amine, A. (2018). Ultrasound assisted magnetic imprinted polymer combined sensor based on carbon black and gold nanoparticles for selective and sensitive electrochemical detection of Bisphenol A. *Sens. Actuators B, 276*, 304–312. https://doi.org/10.1016/j.snb.2018.08.092.

Mohammadi, A., Heydari-Bafrooei, E., Foroughi, M. M., & Mohammadi, M. (2020). Electrochemical aptasensor for ultrasensitive detection of PCB77 using thionine-functionalized MoS2-rGO nanohybrid. *Microchemical Journal, 155*, 104747. https://doi.org/10.1016/j.microc.2020.104747.

Nodehi, M., Baghayeri, M., Behazin, R., & Veisi, H. (2021). Electrochemical aptasensor of bisphenol A constructed based on 3D mesoporous structural SBA-15-Met with a thin layer of gold nanoparticles. *Microchem. J., 162*, Article 105825. https://doi.org/10.1016/j.microc.2020.105825.

Qin, J., Shen, J., Xu, X., Yuan, Y., He, G., & Chen, H. (2018). A glassy carbon electrode modified with nitrogen-doped reduced graphene oxide and melamine for ultra-sensitive voltammetric determination of bisphenol A. *Microchimica Acta, 185*, 459. https://doi.org/10.1007/s00604-018-2998-9.

Rajabnejad, S.-H., Badibostan, H., Verdian, A., Karimi, G. R., Fooladi, E., & Feizy, J. (2020). Aptasensors as promising new tools in bisphenol A detection - An invisible pollution in food and environment. *Microchemical Journal, 155*, 104722. https://doi.org/10.1016/j.microc.2020.104722.

Ren, H., An, Z., & Jang, C.-H. (2019). Liquid crystal-based aptamer sensor for sensitive detection of bisphenol A. *Microchemical Journal, 146*, 1064–1071. https://doi.org/10.1016/j.microc.2019.02.019.

Rostamabadi, P. F., & Heydari-Bafrooei, E. (2019). Impedimetric aptasensing of the breast cancer biomarker HER2 using a glassy carbon electrode modified with gold nanoparticles in a composite consisting of electrochemically reduced graphene oxide and single-walled carbon nanotubes. *Microchimica Acta., 186*, 495. https://doi.org/10.1007/s00604-019-3619-y.

Seo, H. B., & Gu, M. B. (2017). Aptamer-based sandwich-type biosensors. *Journal of Biological Engineering, 11*, 11. https://doi.org/10.1186/s13036-017-0054-7.

Singh, P., Parent, K. L., & Buttry, D. A. (2012). Electrochemical Solid-State Phase Transformations of Silver Nanoparticles. *Journal of the American Chemical Society, 134*(12), 5610–5617. https://doi.org/10.1021/ja2109536.

Xu, L., Duan, W., Chen, F., Zhang, J., & Li, H. (2020). A photoelectrochemical aptasensor for the determination of bisphenol A based on the Cu (I) modified graphitic carbon nitride. *J. Hazard. Mater., 400*, Article 123162. https://doi.org/10.1016/j.jhazmat.2020.123162.

Yang, H., Liu, X., Fei, R., & Hu, Y. (2013). Sensitive and selective detection of Ag^{+} in aqueous solutions using Fe_3O_4@Au nanoparticles as smart electrochemical nanosensors. *Talanta, 116*, 548–553. https://doi.org/10.1016/j.talanta.2013.07.041.

Yu, Z., Luan, Y., Li, H., Wang, W., Wang, X., & Zhang, Q. (2019). A disposable electrochemical aptasensor using single-stranded DNA–methylene blue complex as signal-amplification platform for sensitive sensing of bisphenol A. *Sensors and Actuators B, 284*, 73–80. https://doi.org/10.1016/j.snb.2018.12.126.

Yun, W., Wu, H., Chen, L., & Yang, L. (2018). Dual enzyme-free amplification strategy for ultra-sensitive fluorescent detection of bisphenol A in water. *Analytica Chimica Acta, 1020*, 104–109. https://doi.org/10.1016/j.aca.2018.02.064.

Zhang, H., Luo, F., Wang, P., Guo, L., Qiu, B., & Lin, Z. (2019). Signal-on electrochemiluminescence aptasensor for bisphenol A based on hybridization chain reaction and electrically heated electrode. *Biosensors and Bioelectronics, 129*, 36–41. https://doi.org/10.1016/j.bios.2019.01.007.

Zhang, Y., Wang, Z., & Jiang, W. (2011). A sensitive fluorimetric biosensor for detection of DNA hybridization based on Fe/Au core/shell nanoparticles. *Analyst, 136*(4), 702–707. https://doi.org/10.1039/C0AN00583E.

Zhang, Y., Lei, Y., Lu, H., Shi, L., Wang, P., Ali, Z., & Li, J. (2021). Electrochemical detection of bisphenols in food: A review. *Food Chem., 346*, 128895. https://doi.org/10.1016/j.foodchem.2020.128895.

Zhao, Y., Bai, X.-L., Song, T., Zhang, G.-L., Yuan, Y.-C., Liu, Y.-M., & Liao, X. (2019). Determination of environmental estrogens and bisphenol A in water samples by ultra-high performance liquid chromatography coupled to Q-Exactive high resolution mass spectrometry after magnetic solid-phase extraction. *Microchemical Journal, 151*, 104212. https://doi.org/10.1016/j.microc.2019.104212.